

ORIGINAL RESEARCH

Open Access



Casson rheological flow model in an inclined stenosed artery with non-Darcian porous medium and quadratic thermal convection

J. U. Abubakar^{*} , Q. A. Omolesho, K. A. Bello and A. M. Basambo

^{*}Correspondence:
abubakar.ju@unilorin.edu.ng

Department of Mathematics,
University of Ilorin, Ilorin, Nigeria

Abstract

The current study investigates the combined response of the Darcy–Brinkman–Forchheimer and nonlinear thermal convection influence among other fluid parameters on Casson rheology (blood) flow through an inclined tapered stenosed artery with magnetic effect. Considering the remarkable importance of mathematical models to the physical behavior of fluid flow in human systems for scientific, biological, and industrial use, the present model predicts the motion and heat transfer of blood flow through tapered stenosed arteries under some underline conditions. The momentum and energy equations for the model were obtained and solved using the collocation method with the Legendre polynomial basis function. The expressions obtained for the velocity and temperature were graphed to show the effects of the Darcy–Brinkman–Forchheimer term, Casson parameters, and nonlinear thermal convection term among others. The results identified that a higher Darcy–Brinkman number slows down the blood temperature, while continuous injection of the Casson number decreases both velocity and temperature distribution.

Keywords: Casson fluid, Inclined stenosed artery, Magnetohydrodynamics (MHD) fluid, Collocation method, Darcy–Brinkman–Forchheimer

Mathematics Subject Classification: 76A05, 76D05, 76Z05

Introduction

Stenosis refers to a strange narrowing in a blood vessel or other tubular organs such as the foramina and canal. It is also known as urethral stricture. Atherosclerosis is the majorly cause of stenosis, a form of the disease in which the wall of the artery develops lesions (abnormalities that can eventually lead to narrowing due to deposits of fats). Blood is a non-Newtonian fluid, that is, the viscosity varies with the shear rate which makes it a shear-thinning fluid. The study of mathematical biology and computational fluid mechanics has enhanced the work of researchers to inspect the mathematical and physical behavior of blood flow for use in medicine and other industrial applications. Among the novel, investigations in the area of tapered stenosed arteries include the work of Abubakar and Adeoye [2], and Abubakar et al. [1] study of steady blood flow through stenosis under the influence of a magnetic field. The influence of MHD blood

flow and heat transfer through an inclined porous stenosed artery with variable viscosity is presented by Tripathi and Kumar [19]. Chaturani and Samy [7] discussed the pulsatile flow of Casson fluid through arteries (stenosed) with blood application. Bio-inspired peristaltic propulsion of hybrid nanofluid flow with hybrid nanoparticle aggregation was discussed by Bhatti et al. [6].

Recently, Sharma et al. [18] investigated the flow of blood through a multi-stenosed tapered artery; the study was centered on the slip flow and thermal radiation influence with the inclusion of hybrid nanoparticles (Au-Al₂O₃/Blood) and second law analysis; thus, the impact of Au and slip velocity is fully remarked. Poonam et al. [17] utilized the finite difference (C-N) scheme to examine the heat and mass transfer flow of pulsatile blood through a curved artery subject to hybrid nanoparticles (Au-Al₂O₃/blood) aggregation, and Ikbar et al. [11] enumerated their model for the non-Newtonian flow of blood through a stenosed artery in the presence of a transverse magnetic field. Blood is taken into account as the third-grade non-Newtonian fluid in the work presented by Akbarzadeh [3]; the study revealed that the mean value of the velocity increases, and the amplitude of the velocity remains constant as the pressure gradient rises.

Mandal et al. [15] developed and discussed a two-dimensional mathematical model for the study of body acceleration external effect on non-Newtonian blood flow in a stenosed artery, and the blood is characterized by the generalized power-law model. Hayat et al. [10] considered Darcy–Brinkman–Forchheimer flow with Cattaneo–Christov homogeneous–heterogeneous, therein, MHD effects are considered on the flow of blood in the stenosed artery. Bio-inspired peristaltic propulsion of hybrid nanofluid flow nanoparticles subject to magnetic effects is carried out by Bhatti and Abdelsalam [6], and their focus demonstrated how Ta-NPs can be employed for the removal of unwanted reactive oxygen species in both small and large animals as well as in biomedical systems. Krishna [12, 13] studied the effect of heat and mass flux conditions on the magnetohydrodynamics flow of Casson fluid over a curved stretching surface. Mustafa [16] investigate the pipe flow of Eyring–Powell fluid enumerating its impact on flow and heat transfer. Mustafa [20] as well study the second law phenomena in thermal transport through the metallic porous channel; in the study, the impact of Brinkman–Darcy model is enumerated, to mention but a few among the numerous investigations. Hemodynamic characteristics of gold nanoparticle blood flow through a tapered stenosed vessel with variable nanofluid viscosity were discussed by Elnaqeeb et al [8]. Beckermann et al. [4] presented the numerical study of a porous enclosure medium with non-Darcian natural convection influence. The work enumerated that Forchheimer’s extension must be included for Prandtl number less than one. In related work, Bhargava et al. [5] explore the finite element analysis for drug diffusion and transient pulsatile magneto-hemodynamic non-Newtonian flow in a porous channel.

Numerical methods have been the simplest and most approachable way of obtaining an approximate solution to systems of highly nonlinear equations of which the collocation method is one of them. The current investigation utilized one of the orthogonal polynomials called the Legendre polynomial combined with the collocation method. Among the studies that have used this approach include Mallawi

et al. [14] solution to the nonlinear differential equation was solved by computational means of Legendre collocation points. Guner and Yalcinbas [9] worked on the Legendre collocation method for solving a nonlinear differential equation, to mention but just a few. Motivated by all the above-mentioned research, this article presents the effects of the non-Darcian porous medium and quadratic thermal convection behavior on equations governing the blood flow through an inclined tapered stenosed artery. The model of the nonlinear equations has been solved numerically using the Legendre collocation method with the aid of Wolfram Mathematica 11.3 under the defined boundary conditions. MAPLE 18 generated the codes are used to show the effects of the Darcy–Brinkman–Forchheimer term, Casson parameters, nonlinear thermal convection term, and variation in inclination angle of the blood flow in the inclined stenosed artery graphically.

Problem formulation

The flow of blood is taken to be flowing in a cylindrical form of the narrow artery, in an axial direction, as shown in Fig. 1. Let $(r, \theta,$ and $z)$ be the polar coordinate system (cylindrical), and let \tilde{u}, \tilde{v} and \tilde{w} be the velocity components in the $r, \theta,$ and z directions. We consider magnetohydrodynamics (MHD) Newtonian fluid of density ρ and variable viscosity μ flowing through a porous material in a tube having a finite length L . The stenosed artery is inclined at the angle γ from the vertical axis with outside applied radiation q_r and magnetic field M .

The governing equations for the model are as follows:

Continuity equation

$$\frac{\partial \tilde{u}}{\partial \tilde{r}} + \frac{\partial \tilde{v}}{\partial \tilde{z}} + \frac{\tilde{u}}{\tilde{r}} = 0 \tag{1}$$

Momentum equation (r -direction)

$$\rho \left[\tilde{u} \frac{\partial \tilde{u}}{\partial \tilde{r}} + \tilde{v} \frac{\partial \tilde{u}}{\partial \tilde{z}} \right] = - \frac{\partial \tilde{P}}{\partial \tilde{r}} + \frac{\partial}{\partial \tilde{r}} \left[2\mu \frac{\partial \tilde{u}}{\partial \tilde{r}} \right] + \frac{2\mu}{\tilde{r}} \left[\frac{\partial \tilde{u}}{\partial \tilde{r}} - \frac{\tilde{u}}{\tilde{r}} \right] + \frac{\partial}{\partial \tilde{z}} \left[\mu \left(\frac{\partial \tilde{u}}{\partial \tilde{z}} + \frac{\partial \tilde{v}}{\partial \tilde{r}} \right) \right] \tag{2}$$

Momentum equation (z -direction)

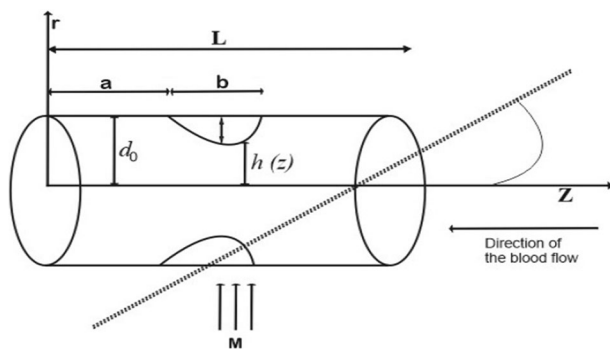


Fig. 1 Geometry of the inclined stenosed artery

$$\begin{aligned} \rho \left[\tilde{u} \frac{\partial \tilde{v}}{\partial \tilde{r}} + \tilde{v} \frac{\partial \tilde{v}}{\partial \tilde{z}} \right] &= -\frac{\partial \tilde{P}}{\partial \tilde{z}} + \left(1 + \frac{1}{\beta} \right) \left\{ \frac{\partial}{\partial \tilde{z}} \left[\left(2\mu \frac{\partial \tilde{v}}{\partial \tilde{z}} \right) \right] + \frac{1}{\tilde{r}} \frac{\partial}{\partial \tilde{r}} \left[\mu \left(\frac{\partial \tilde{u}}{\partial \tilde{z}} + \frac{\partial \tilde{v}}{\partial \tilde{r}} \right) \right] \right\} - \sigma_1 \mu_m^2 H_0^2 \tilde{v} \\ &+ \rho g [\alpha_1 (T - T_0) + \alpha_2 (T - T_0)^2] \cos \gamma - \left(1 + \frac{1}{\beta} \right) \frac{\mu \tilde{V}}{K_1} - \frac{b^* \nu^2}{k_1} \end{aligned} \tag{3}$$

Energy equation

$$\begin{aligned} \rho c_p \left[\tilde{u} \frac{\partial T}{\partial \tilde{r}} + \tilde{v} \frac{\partial T}{\partial \tilde{r}} \right] &= \frac{k}{\tilde{r}} \frac{\partial}{\partial \tilde{r}} \left[\tilde{r} \frac{\partial T}{\partial \tilde{r}} \right] + k \frac{\partial^2 T}{\partial \tilde{z}^2} \\ &+ 2\mu \left(1 + \frac{1}{\beta} \right) + \left\{ \left[\left(\frac{\partial \tilde{u}}{\partial \tilde{z}} \right)^2 + \left(\frac{\tilde{u}}{\tilde{r}} \right)^2 + \left(\frac{\partial \tilde{v}}{\partial \tilde{z}} \right)^2 \right] + \mu \left(\frac{\partial \tilde{u}}{\partial \tilde{z}} + \frac{\partial \tilde{v}}{\partial \tilde{r}} \right)^2 \right\} - \frac{\partial q_r}{\partial \tilde{r}} \end{aligned} \tag{4}$$

where $\frac{b^* \nu^2}{k_1}$ is the Darcy–Forchheimer’s term, \tilde{u} , \tilde{v} , and \tilde{w} are the velocity components in the radial and axial directions, respectively. σ_1 is the electrical conductivity, k is the thermal conductivity, and C_p is the specific heat at constant pressure. The differential equation for the radiative flux q_r is given in the following equation:

$$\frac{\partial^2 q_r}{\partial \tilde{r}^2} - 3\alpha_v^2 q_r - 16\alpha_v \sigma T^3 \frac{\partial T}{\partial \tilde{r}} = 0, \tag{5}$$

where σ is the Stefan–Boltzmann constant. With the assumption of thin blood, $\alpha_v \ll 1$. Then, T_0 is the blood temperature at the stenosed region and T is the local temperature of the blood, then (5) can be solved to

$$\frac{\partial q_r}{\partial \tilde{r}} = 4\alpha_v^2 (T - T_0), \tag{6}$$

The variable viscosity of the flow of blood is expressed by the formula:

$$\mu(\tilde{r}) = \mu_0 (\lambda h(\tilde{r}) + 1), \tag{7}$$

where $h(\tilde{r}) = H \left[1 - \left(\frac{\tilde{r}}{d_0} \right)^m \right]$ and $H_r = \lambda H$ in which λ is having a numerical value of 2.5 and H is the maximum hematocrit at the center of the artery, m is the parameter that decides the exact shape of the blood velocity profile and H_r is the hematocrit parameter. The geometry illustration of the stenosis located at the point, z with its maximum height, δ is defined by the following formula:

$$\begin{aligned} h(\tilde{z}) &= \left[1 - \eta \left(b^{n-1} (\tilde{z} - a) - (\tilde{z} - a)^n \right) \right] d(\tilde{z}), \\ &\text{where } a \leq \tilde{z} \leq a + b, \quad h(\tilde{z}) = d(\tilde{z}), \text{ otherwise,} \end{aligned} \tag{8}$$

where $d(\tilde{z})$ is the radius of the narrow artery in the stenotic region with $d(\tilde{z}) = d_0 + \xi \tilde{z}$, In (8), n is the shape parameter which determines the shape of the constriction profile. The value $n = 2$ results in symmetrically shaped stenosis, and for nonsymmetric stenosis case n considers the values $n \geq 2$. ξ is the narrowed parameter defined by $\xi = \tan \varphi$, where φ is known as narrowed artery and ξ as the narrowing parameter which is defined by the case of converging, and d_0 is the radius of the non-narrowed artery.

The parameter η is defined as

$$\eta = \frac{\delta^* n^{\frac{n}{n-1}}}{d_0 b^n (n-1)} \tag{9}$$

where δ is the maximum height of the stenosis located at

$$\tilde{z} = a + \frac{b}{n^{\frac{n}{n-1}}}. \tag{10}$$

Method of solution

To non-dimensionalize the obtained governing equations, we introduce the non-dimensional variables as follows:

$$\begin{aligned} \tilde{u} &= \frac{uu_0\delta}{b}, \quad \tilde{r} = rd_0, \quad \tilde{z} = zb, \quad \tilde{v} = wu_0, \quad \tilde{h} = hd_0, \quad \tilde{P} = \frac{u_0 b \mu_0 p}{d_0^2}, \\ \text{Re} &= \frac{\rho b u_0}{\mu_0}, \quad \theta = \frac{T - T_0}{T_0}, \quad \text{Pr} = \frac{\mu c_p}{k}, \quad \text{Ec} = \frac{\mu_0^2}{c_p T_0}, \quad Z = \frac{k_1}{d_0^2}, \\ M &= \frac{\sigma_1 H_0^2 d_0^2}{\mu_0}, \quad Q = A \frac{d_0^2}{K}, \quad G_r = \frac{g \alpha d_0^3 T_0}{\nu^2}, \quad N^2 = \frac{4 d_0^2 \alpha_v^2}{k}, \quad G_N = \frac{\alpha_2}{\alpha_1} T_0. \end{aligned} \tag{11}$$

where Pr , Z , N , Re , θ , Z , Gr , M , Ec and G_N , respectively, represent the Prandtl number, porosity parameter, radiation absorption parameter, Reynolds number, temperature parameter, Grashof number, magnetic field parameter, Eckert number, and non-linear thermal convection. In the case of aortic stenosis $\frac{\delta}{d_0} \ll 1$ and the other additional conditions,

$$\text{Re} \frac{\delta^* n^{\frac{1}{n-1}}}{b} = 1, \tag{12}$$

assuming the following approximation:

$$\frac{d_0 n^{\frac{1}{n-1}}}{b} \sim O(1), \tag{13}$$

To non-dimensionalize the continuity equation, we substitute the non-dimensional quantities in (11) into (1) to obtain:

$$\frac{u_0 \delta}{b d_0} \frac{\partial u}{\partial r} + \frac{u u_0 \delta}{r b d_0} + \frac{u_0}{b} \frac{\partial w}{\partial z} = 0, \tag{14}$$

Since $\frac{\delta}{d_0} = 1$,

$$\frac{u_0}{b} \frac{\partial w}{\partial z} = 0, \tag{15}$$

$$\frac{\partial w}{\partial z} = 0. \tag{16}$$

To non-dimensionalize the momentum equation (r -direction), substitute (11) into (2) to obtain:

Also, since $\frac{\delta}{d_0} = 1, \frac{\partial w}{\partial z} = 0,$

$$-\frac{u_0 b \mu_0}{d_0^3} \frac{\partial p}{\partial z} = 0, \tag{17}$$

$$\frac{\partial p}{\partial z} = 0. \tag{18}$$

Also, substituting the non-dimensional variables in (11) and (7) into the momentum equation (z-direction):

$$\begin{aligned} \frac{\partial p}{\partial z} = & \left(1 + \frac{1}{\beta}\right) \left[H_r \left(\frac{1}{r} - r^{m-1} (m+1) \right) \right] \frac{\partial w}{\partial r} + \left(1 + \frac{1}{\beta}\right) [1 + H_r (1 - r^m)] \frac{\partial^2 w}{\partial r^2} w M^2 \\ & + G_r [\theta + G_N \theta^2] \cos \gamma - w \left(1 + \frac{1}{\beta}\right) \frac{H_r}{Z} (1 - r^m) - \frac{b^* w^2 d_0^2}{k_1}, \end{aligned} \tag{19}$$

where $G_N = \frac{\alpha_2 T_0}{\alpha_1}$ is the nonlinear thermal convection.

Also, using the non-dimensional variables in Eq. (11), the energy equation becomes

$$\frac{1}{r} \frac{\partial}{\partial r} \left(r \frac{\partial \theta}{\partial r} \right) + Ec Pr \left(1 + \frac{1}{\beta} \right) [1 + H_r (1 - r^m)] \left(\frac{\partial w}{\partial r} \right)^2 - N^2 \theta = 0, \tag{20}$$

where $B_r = Ec Pr$ Brinkman number (B_r) is a dimensionless number used to study viscous flow. The corresponding boundary conditions are

$$\frac{\partial \theta}{\partial r} = 0, \quad \frac{\partial w}{\partial r} = 0, \quad \text{at } r = 0, \tag{21}$$

and the no-slip boundary conditions (assuming that at a solid boundary, the fluid will have zero velocity relative to the boundary) at the artery wall

$$w = 0, \quad \theta = 0, \quad \text{at } r = h(z), \tag{22}$$

where $h(z)$ is defined by

$$\begin{aligned} h(z) = & (1 + \xi' z) [1 - \eta_1 ((z - a') - (z - a')^n)], \\ & \text{where } a' \leq z \leq a' + 1 \end{aligned} \tag{23}$$

With the use of the Legendre collocation method, we have to define some functions. Let $P_n(x)$ be the Legendre polynomial function of degree n . We recall that $P(x)$ is the solution (eigenfunction) of the Sturm–Liouville problem as follows:

$$\begin{aligned} \left[(1 - x^2) P_n'(x) \right]' + n(n+1) P_n(x) = 0, \\ x \in [-1, 1], \quad n = 0, 1, 2, 3, \dots \end{aligned} \tag{24}$$

Equation (24) satisfies the recursive relations:

$$P_0(x) = 1, P_1(x) = x, P_2(x) = \frac{1}{2}(3x^2 - 1), \tag{25}$$

$$P_n(x) = \frac{2n - 1}{n} x P_{n-1}(x) - \frac{n - 1}{n} P_{n-2}(x); n \geq 1, \tag{26}$$

The set of Legendre polynomials from a $[-1, 1]$ orthogonal set is

$$\int_{-1}^1 P_n(x)P_m(x) w(x)dx = \frac{2}{2n + 1} \delta_{m,n}, \tag{27}$$

where $\delta_{m,n}$ is the Kronecker delta function. To apply the Legendre polynomial to the problem with a semi-infinite domain, we introduce algebraic mapping

$$x = \frac{2\zeta}{h} - 1, [-1, 1] \rightarrow [0, h], \tag{28}$$

the boundary value problem is solved within the region $[0, h]$ in place of $[0, \infty)$, whereas the scaling parameter is taken to be sufficiently large enough to evaluate the thickness of the boundary layer. Therefore, the real solutions $f(\zeta)$ and $\theta(\zeta)$ are expressed as the basis of the Legendre polynomial function as

$$f(\zeta) = \sum_{j=0}^N a_j P_j(\zeta), \quad \theta(\zeta) = \sum_{j=0}^N b_j P_j(\zeta), \quad \text{for } j = 0, 1, 2, 3, \dots, \tag{29}$$

Hence,

$$\begin{aligned} f(\zeta) &= a_0 P_0(\zeta) + a_1 P_1(\zeta) + a_2 P_2(\zeta) + \dots, \\ \theta(\zeta) &= b_0 P_0(\zeta) + b_1 P_1(\zeta) + b_2 P_2(\zeta) + \dots, \end{aligned} \tag{30}$$

where $P_0(\zeta), P_1(\zeta), P_2(\zeta), \dots, P_n(\zeta)$ are generated from recursive relation in (26) and

$$P_0(\zeta) = 1, P_1(\zeta) = \zeta, P_2(\zeta) = \frac{1}{2}(3\zeta^2 - 1), \dots \tag{31}$$

Hence, substituting Eq. (31) into (30)

$$f(\zeta) = a_0 + a_1 \left(\frac{2\zeta}{h} - 1 \right) + \frac{a_2}{2} \left[3 \left(\frac{2\zeta}{h} - 1 \right)^2 - 1 \right] + \dots, \tag{32}$$

$$\theta(\zeta) = b_0 + b_1 \left(\frac{2\zeta}{h} - 1 \right) + \frac{b_2}{2} \left[3 \left(\frac{2\zeta}{h} - 1 \right)^2 - 1 \right] + \dots, \tag{33}$$

for $h = 6$ and $N = 6$, Eqs. (32–33) become

$$f(\zeta) = a_0 + \frac{a_1}{6}(-6 + 2\zeta) + \frac{a_2}{6}[6 - 6\zeta + \zeta^2] + \dots \tag{34}$$

$$\theta(\zeta) = b_0 + \frac{b_1}{6}(-6 + 2\zeta) + \frac{b_2}{6}[6 - 6\zeta + \zeta^2] + \dots \tag{35}$$

We assumed that $w(r)$ and $\theta(r)$ are the Legendre base trial functions, defined by

$$w(z) = \sum_{j=0}^N a_j P_j \left(\frac{2z}{h} - 1 \right), \quad \theta(r) = \sum_{j=0}^N b_j P_j \left(\frac{2r}{h} - 1 \right), \tag{36}$$

where a_j and b_j are constants to be determined and $P_j \left(\frac{2r}{h} - 1 \right)$ is the shifted Legendre function from $[-1, 1]$ to $[0, h]$. Substituting (36) into the boundary conditions in (21) and (22), respectively, we have

$$\left[\frac{d}{dr} \sum_{j=0}^N a_j P_j \left(\frac{2r}{h} - 1 \right) \right]_{r=0} = 0, \quad \left[\frac{d}{dr} \sum_{j=0}^N b_j P_j \left(\frac{2r}{h} - 1 \right) \right]_{r=0} = 0, \tag{37}$$

$$\left[\sum_{j=0}^N a_j P_j \left(\frac{2r}{h} - 1 \right) \right]_{r=h(z)} = 0, \quad \left[\sum_{j=0}^N b_j P_j \left(\frac{2r}{h} - 1 \right) \right]_{r=h(z)} = 0, \tag{38}$$

Residues $D_w(r, a_j, b_j)$ and $D_\theta(r, a_j, b_j)$ are derived from the above (39) and (40) accordingly.

The residues are minimized close to zero using the collocation method as follows:

$$\text{for } \delta(r - r_j) = \begin{cases} 1, & t = t_j \\ 0, & \text{otherwise,} \end{cases}$$

$$\int_0^1 D_w \delta(r - r_j) dr = D_f(r_j, a_k, b_k) = 0, \quad \text{for } j = 1, 2, \dots, N - 1 \tag{39}$$

$$\int_0^1 D_\theta \delta(r - r_j) dr = D_\theta(r_j, a_k, b_k) = 0, \quad \text{for } j = 1, 2, \dots, N - 1 \tag{40}$$

The above procedure sought the unknown constant coefficients a_j , and b_j which are then substituted in Eq. (36) as the required solution.

Results and discussion

Mathematica 11.3 is used to obtain the numerical results for the temperature and velocity variation. The parameters used include the inclination of the angle (γ) of the artery, Casson parameter (β), porosity parameter (Z), the height of the stenosis (δ), Darcy–Brinkman–Forchheimer term (F_s), and nonlinear thermal convection term (G_n). The following various parameters were used in the plotting of the graphs. $z = 0.5, \delta = 0.1, N = 1.5, \gamma = \frac{\pi}{3}, a = 0.25, b = 1, \xi = 0.002, Ec = 1, P_r = 2, Gr = 2, n = 2, h = 0.92, \frac{\partial P}{\partial z} = 3, H_r = 1$ and $d_0 = 1$.

Figure 2a shows the effects of variation of inclination angle (γ) parameters on the velocity profile. There is an increase in the velocity of the blood flow in the artery as the angle of inclination (γ) values increase.

Figure 2b displays the graphical features of the introduced nonlinear thermal convection parameter (G_N) on the velocity profile. It is seen from Fig. 2b that the velocity profile decreases with the increasing values of the nonlinear thermal convection parameter

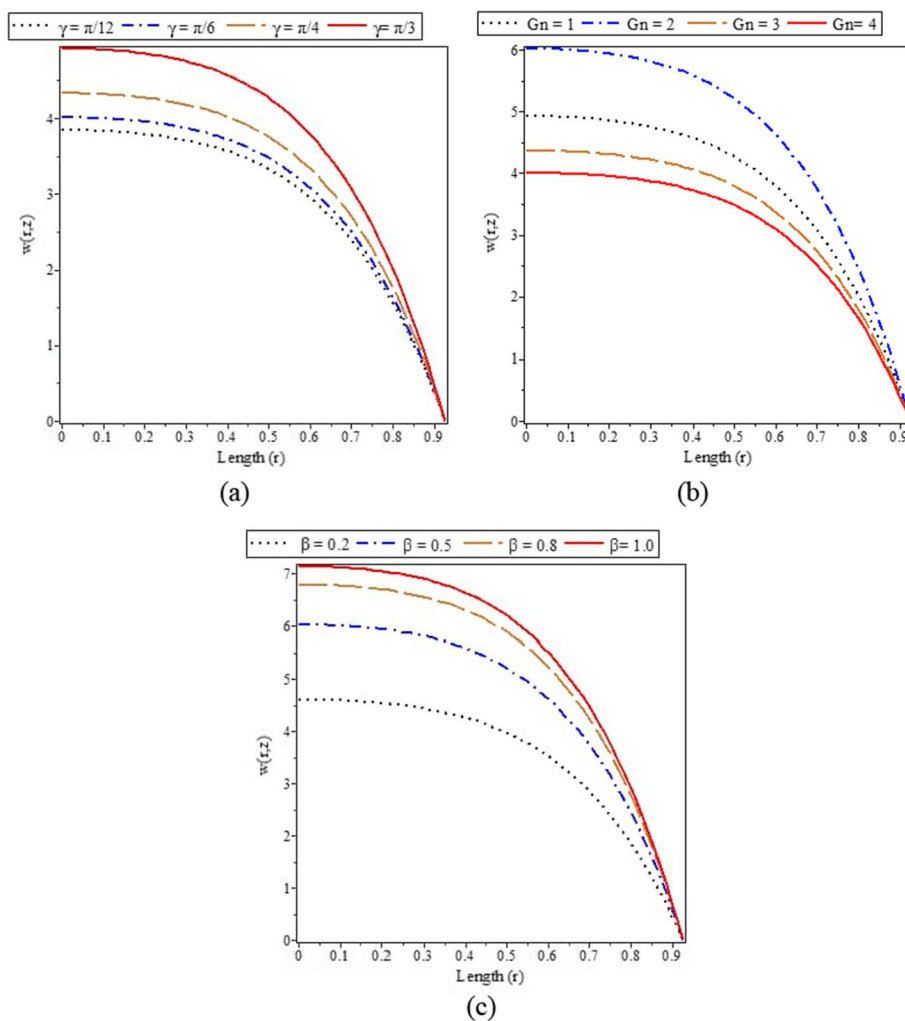


Fig. 2 Influence of Inclination angle (γ), nonlinear thermal convection term (G_N), and Casson parameter on the velocity profile

(G_N). Figure 2c depicts the effect of the scale of the Casson parameter (β); it shows that as it increases from 0.2 to 1.0, velocity increases at the arterial wall.

Figure 3a shows the effects of variation of the inclination angle parameter (γ), on the temperature profile. There is an increase in the temperature of the blood flow in the artery as the inclination angle (γ) values increase.

From Fig. 3b, it is clear that as the value of the nonlinear thermal convection parameter increases, the temperature profile decreases, respectively. It is observed through these figures that velocity and temperature achieve their maximum value at the wall of the artery and attain the minimum value at the middle of the artery for the nonlinear thermal convection parameter. From Fig. 3c, it is seen that as the value of the Casson parameter (β) increases, the temperature profile decreases at the arterial wall and this takes place maybe because of the viscous nature of the fluid which decreases with increasing values of temperature.

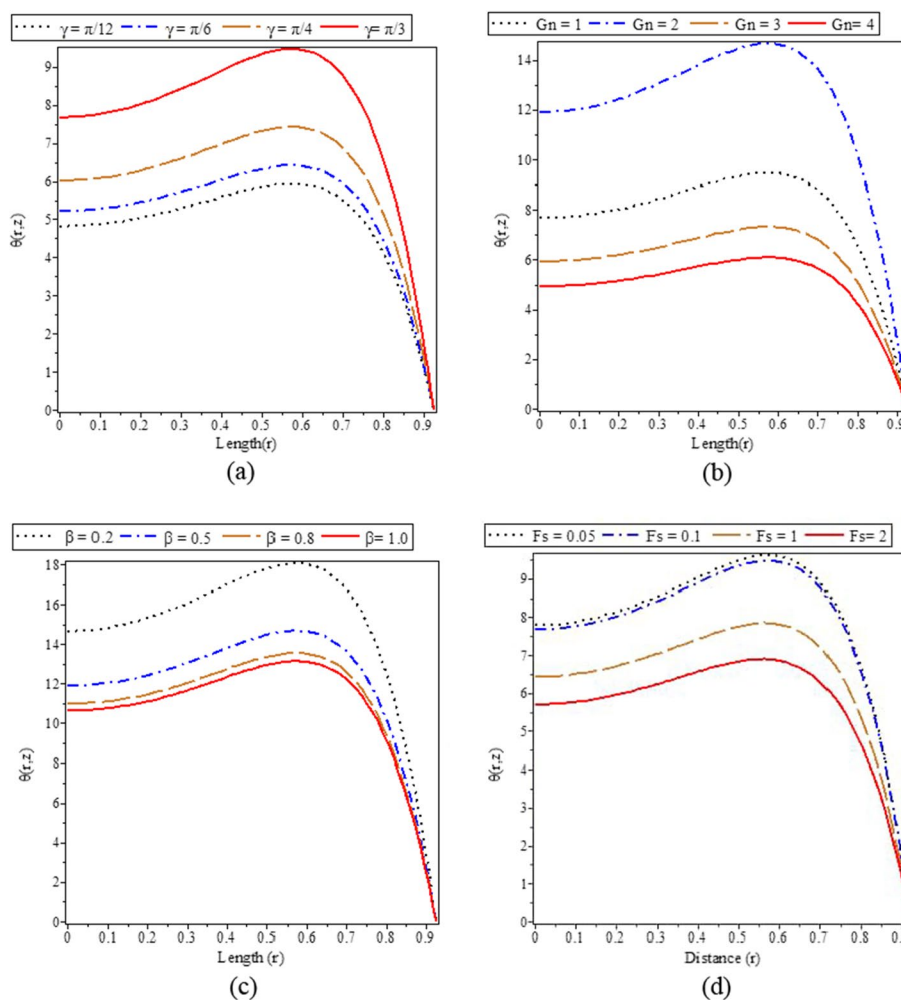


Fig. 3 Influence of **a** inclination angle (γ), **b** nonlinear thermal convection (G_N), **c** Casson parameter, and **d** Darcy–Brinkman–Forchheimer on the temperature profile

Conclusion

In this paper, we studied the Casson rheological flow of blood in an inclined stenosed artery with a non-Darcian porous medium and quadratic thermal convection. The collocation method with Legendre polynomial basis functions was used to solve the nonlinear governing equations. From the velocity and temperature profiles, it concluded that: (i) as the angle of inclination parameter (γ) increases both the blood flow velocity and temperature increase, (ii) with an increase in the value of nonlinear thermal convection parameter (G_N) the velocity and the temperature of the blood flow also increase, and (iii) the increase in Casson parameter (β) gives a decrease on both velocity and temperature of the blood flow.

Appendix 1

Also, on substituting (38) into the governing Eq. (20), we obtain

$$\begin{aligned}
 D_w := & \left(1 + \frac{1}{\beta}\right) \left[H_r \left(\frac{1}{r} - (m+1)r^{m-1} \right) \right] \left[\frac{d}{dr} \sum_{j=0}^N b_j P_j \left(\frac{2r}{h} - 1 \right) \right] \\
 & + \left(1 + \frac{1}{\beta}\right) [1 + H_r(1 - r^m)] \frac{d^2}{dr^2} \left[\sum_{j=0}^N b_j P_j \left(\frac{2r}{h} - 1 \right) \right] \\
 & - \left(\sum_{j=0}^N b_j P_j \left(\frac{2r}{h} - 1 \right) \right) M^2 + G_r \left[\sum_{j=0}^N c_j P_j \left(\frac{2r}{h} - 1 \right) \right. \\
 & \left. + G_N \left(\sum_{j=0}^N c_j P_j \left(\frac{2r}{h} - 1 \right) \right)^2 \right] \cos \gamma - \left(\sum_{j=0}^N b_j P_j \left(\frac{2r}{h} - 1 \right) \right) \\
 & + \left(1 + \frac{1}{\beta}\right) \frac{H_r}{Z} (1 - r^m) - \frac{b^* \left(\sum_{j=0}^N b_j P_j \left(\frac{2r}{h} - 1 \right) \right)^2 d_0^2}{k_1} - \frac{d}{dz} \sum_{j=0}^N a_j P_j \left(\frac{2z}{h} - 1 \right),
 \end{aligned} \tag{41}$$

$$\begin{aligned}
 D_\theta := & \frac{1}{r} \frac{d}{dr} \left(r \frac{d}{dr} \sum_{j=0}^N c_j P_j \left(\frac{2r}{h} - 1 \right) \right) + E_c P_r \left(1 + \frac{1}{\beta} \right) [1 + H_r(1 - r^m)] \\
 & \times \left(\frac{d}{dr} \sum_{j=0}^N c_j P_j \left(\frac{2r}{h} - 1 \right) \right)^2 - N^2 \left(\sum_{j=0}^N c_j P_j \left(\frac{2r}{h} - 1 \right) \right).
 \end{aligned} \tag{42}$$

List of symbols

- \vec{u}, \vec{v} and \vec{w} Velocity components in the r, θ , and z directions
- ρ Variable viscosity
- γ Inclined at the angle
- μ Variable viscosity
- L Tube length
- q_r Applied radiation
- M Magnetic field
- σ_1 Electrical conductivity
- k Thermal conductivity
- C_p Specific heat at constant pressure
- T_0 Blood temperature at the stenosed region
- T Local temperature of the blood
- H Maximum hematocrit at the center of the artery
- H_r Hematocrit parameter
- $d(\bar{z})$ Radius of the narrow artery in the stenotic region
- d_0 Radius of the non-narrowed artery
- δ Maximum height of the stenosis
- Pr Prandtl number
- Z Porosity parameter
- N Radiation absorption parameter
- Re Reynolds number
- θ Dimensionless temperature parameter
- Gr Grashof number
- Ec Eckert number
- G_N Nonlinear thermal convection parameter
- f Dimensionless fluid velocity

Acknowledgements

Not applicable.

Author contributions

JUA and QAO formulate the model and JUA, QAO, KAB, and AMB solved the model, drew the graphs presented, discussed the results, and presented the conclusions. All authors read and approved the final manuscript.

Funding

It was funded by authors.

Availability of data and materials

Not applicable.

Declarations**Competing interests**

We, the authors, declare that there are no competing interests.

Received: 13 December 2021 Accepted: 29 November 2022

Published online: 23 December 2022

References

1. Abubakar, J.U., Gbedeyan, J.A., Ojo, J.B.: Steady blood flow through vascular stenosis under the influence of magnetic field. *Centrepoint J. (Sci. Ed.)* **25**(1), 61–82 (2019)
2. Abubakar, J.U., Adeoye, A.D.: Effects of radiative heat and magnetic field on blood flow in an inclined tapered stenosed porous artery. *J. Taibah Univ. Sci.* **14**(1), 77–86 (2020). <https://doi.org/10.1080/16583655.2019.1701397>
3. Akbarzadeh, P.: Pulsatile Magneto-hydrodynamic blood flows through porous blood vessels using a third grade non-newtonian fluids model. *Comput. Methods Progr. Biomed.* **126**(3–19), 2016 (2016)
4. Beckermann, C., Viskanta, R., Ramadhyani, S.: A numerical study of non-Darcian natural convection in a vertical enclosure filled with a porous medium. *Numer. Heat Transf.* **10**, 557–570 (1986)
5. Bhargava, R., Anwar, O., Rawat, S., Beg, T.A., Tripathi, D.: Finite element study of transient pulsatile magneto-hemodynamic non-Newtonian flow and drug diffusion in a porous medium channel. *J. Mech. Med. Biol.* **12**(14), 1250081 (2012)
6. Bhatti, M.M., Abdelsalam, S.I.: Bio-inspired peristaltic propulsion of hybrid nanofluid flow with Tantalum (Ta) and Gold (Au) nanoparticles under magnetic effects. *Waves Random Complex Med.* (2021). <https://doi.org/10.1080/17455030.2021.1998728>
7. Chaturani, P., Samy, R.P.: Pulsative flow of Casson's fluid through stenosed arteries with applications to blood flow. *Biorheology* **23**(5), 499–511 (1986)
8. Elnaqeeb, T., Sheh, N.A., Mekheimer, K.S.: Hemodynamics characteristics of gold nanoparticle blood flow through a tapered stenosed vessel with variable nanofluid viscosity. *BioNanoScience* **9**(2), 245–255 (2019)
9. Guner, A., Yalcinbas, S.: Legendre collocation method for solving nonlinear differential equations. *Math. Comput. Appl.* **18**(3), 521–530 (2013)
10. Hayat, T., Haider, F., Muhammad, T., Alsaedi, A.: Darcy–Forchheimer flow with Cattaneo–Christov homogeneous-heterogeneous. *PLoS ONE* **12**(2017), 1–18 (2017)
11. Ikbar, M.A., Chakravarty, S., Kelvin, K.L., Wong, M.J., Mandal, P.K.: Unsteady response of non-newtonian blood flow through a stenosed artery in magnetic field. *J. Comput. Appl. Math.* **230**(1), 243–259 (2009)
12. Krishna, M.M.: Effect of heat and mass flux conditions on Magneto hydrodynamics flow of Casson fluid over a curved stretching surface (2019). <https://doi.org/10.4028/www.scientific.net/DDF.392.29>
13. Krishna, M.M.: Numerical investigation on magneto hydrodynamics flow of Casson fluid over a deformable porous layer with slip conditions. *Indian J. Phys.* (2019). <https://doi.org/10.1007/s12648-019-01668-4>
14. Mallawi, F., Alzaidy, J.F., Hafez, R.M.: Application of a Legendre collocation method to the space-time variable fractional-order advection-dispersion equation. *J. Taibah Univ. Sci.* **13**, 2019 (2018)
15. Mandal, P.K., Chakravarthy, S., Mandal, A., Amin, N.: Effect of the body acceleration on unsteady pulsatile flow of non-Newtonian fluid through a stenosed artery. *Appl. Math. Comput.* **189**, 766–779 (2007)
16. Mustafa, T.: Eyring–Powell fluid flow through a circular pipe and heat transfer: full solutions. *Int. J. Numer. Meth. Heat Fluid Flow* **30**(11), 4765–4774 (2020). <https://doi.org/10.1108/hff-12-2019-0925>
17. Poonam, Sharma, B.K., Kumawat, C., Vafai, K.: Computational biomedical simulations of hybrid nanoparticles (blood-mediated) transport in a stenosed and aneurysmal curved artery with heat and mass transfer: hematocrit dependent viscosity approach. *Chem. Phys. Lett.* **800**, 139666 (2022)
18. Sharma, B.K., Rishu Gandhi, M.M.: Bhatti, Entropy analysis of thermally radiating MHD slip flow of hybrid nanoparticles (Au–Al₂O₃/Blood) through a tapered multi-stenosed artery. *Chem. Phys. Lett.* **790**, 139348 (2022). <https://doi.org/10.1016/j.cplett.2022.139348>
19. Tripathi, B., Kumar, B.S.: MHD blood flow and heat transfer through an inclined porous stenosed artery with variable viscosity. *J. Taibah Univ. Sci.* **14**(1), 77–86 (2019). <https://doi.org/10.1080/16583655.2019.1701397>
20. Turkyilmazoglu, M.: Velocity slip and entropy generation phenomena in thermal transport through metallic porous channel. *J. Non-Equilib. Thermodyn.* (2020). <https://doi.org/10.1515/jnet-2019-0097>

Publisher's Note

Springer Nature remains neutral with regard to jurisdictional claims in published maps and institutional affiliations.